

Effect of Constrained Donor Atom Orientations on the Stabilities, Complexation Kinetics, Redox Potentials, and Structures of Macrocyclic Polythiaether Complexes. Copper(II) Complexes with Cyclopentanediy Derivatives of [14]aneS₄ in 80% Methanol

Safaa H. Kakos,^{1a} Luke T. Dressel,^{1b} Jeffery D. Bushendorf,^{1b} Casimir P. Kotarba,^{1a} Prabodha Wijetunge,^{1a} Chandrika P. Kulatilleke,^{1a} Michael P. McGillivray,^{1a} Gezahegn Chaka,^{1a} Mary Jane Heeg,^{1a} L. A. Ochrymowycz,^{1b} and D. B. Rorabacher*,^{1a}

Department of Chemistry, Wayne State University, Detroit, Michigan 48202, and Department of Chemistry, University of Wisconsin, Eau Claire, Wisconsin 54701

Received September 28, 2005

The two ethylene bridges in the macrocyclic tetrathiaether 1,4,8,11-tetrathiacyclotetradecane ([14]aneS₄) have been systematically replaced by *cis*- or *trans*-1,2-cyclopentane to generate a series of new ligands that exhibit differing preferences for the orientation of the sulfur donor atoms while maintaining constant inductive effects. The resulting five dicyclopentanediy derivatives, along with two previously synthesized monocyclopentanediy analogues, have been complexed with Cu^{II}, and their stability constants, formation and dissociation rate constants, and redox potentials have been determined in 80% methanol/20% water (by weight). The crystal structures of the Cu^{II} complexes with the five dicyclopentanediy-[14]aneS₄ diastereomers as well as the structures for a representative Cu^I complex and one of the free ligands have also been determined. The properties of these complexes are compared to previous data obtained for the corresponding cyclohexanediy derivatives in an attempt to shed additional light on the influence of sterically constraining substituents upon the properties of macrocyclic ligand complexes.

Introduction

The term “macrocyclic effect” was coined by Cabiness and Margerum² to describe the observed increase in stability constants for metal ion complexes involving macrocyclic ligands compared to corresponding acyclic ligands. Hinz and Margerum³ subsequently reported a macrocyclic enhancement of greater than 10⁶ in the stability constants for aqueous Ni^{II} reacting with unsubstituted macrocyclic and acyclic tetramines. They noted that the uncomplexed macrocyclic tetramines tend preferentially to adopt an endo conformation in which the nitrogen donor atoms are preoriented toward the ligand cavity, thereby making them less accessible to the surrounding aqueous solvent compared to similar acyclic ligands. Thus, they hypothesized that their observed “macrocyclic effect” was largely an enthalpy effect because, for

the macrocycle, less energy is required to overcome hydrogen bonding between the nitrogen donor atoms and the solvent, a hypothesis later substantiated by Clay, Paoletti and co-workers.⁴ In their study, Hinz and Margerum also noted that the macrocyclic enhancement was *reduced* by a factor of from 2 to 10⁴ when methyl groups were sequentially substituted on the periphery of the parent macrocyclic tetramine.

In contrast to the tetramine macrocycles, uncomplexed macrocyclic tetrathiaethers tend to adopt an exo conformation in which the lone electron pairs on the donor atoms are oriented away from the ligand cavity.^{5,6} Thus, metal ion complexation requires the rotation of the donor atoms into an endo conformer, an unfavorable entropic contribution.⁷

* To whom correspondence should be addressed. E-mail: dbr@chem.wayne.edu. Fax: (313) 577-8822.

(1) (a) Wayne State University. (b) University of Wisconsin.

(2) Cabiness, D. K.; Margerum, D. W. *J. Am. Chem. Soc.* **1969**, *91*, 6540–6541.

(3) Hinz, F. P.; Margerum, D. W. *Inorg. Chem.* **1974**, *13*, 2941–2949.

(4) Clay, R. M.; Micheloni, M.; Paoletti, P.; Steele, W. V. *J. Am. Chem. Soc.* **1979**, *101*, 4119–4122.

(5) DeSimone, R. E.; Glick, M. D. *J. Am. Chem. Soc.* **1976**, *98*, 762–767.

(6) (a) Cooper, S. R.; Rawles, S. C. *Struct. Bonding (Berlin)* **1990**, *72*, 1–72. (b) Blake, A. J.; Schröder, M. *Adv. Inorg. Chem.* **1990**, *35*, 1–80.

(7) Sokol, L. S. W. L.; Ochrymowycz, L. A.; Rorabacher, D. B. *Inorg. Chem.* **1981**, *20*, 3189–3195.

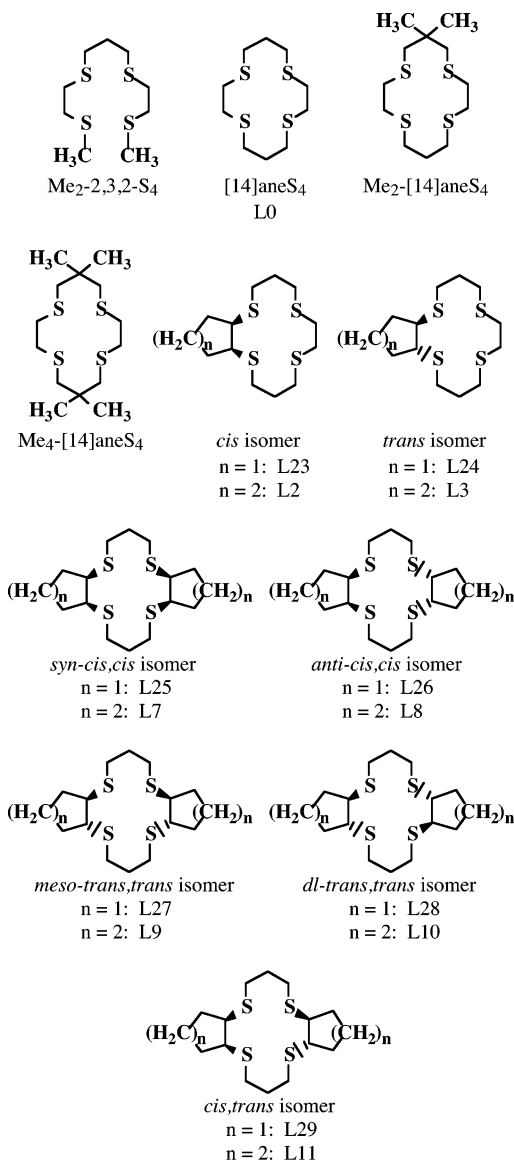


Figure 1. Ligands discussed in this work.

In combination with weaker donor atom–solvent interactions, the macrocyclic effect for unsubstituted tetrathiaethers is only about 10^2 , as determined from the comparative stabilities of Cu^{II} complexes with unsubstituted acyclic and macrocyclic tetrathiaethers (Me_2 -2,3,2- S_4 and [14]ane S_4 ; see Figure 1).⁷ In opposition to the tetramine behavior, Desper and Gellman^{8,9} found that the substitution of *gem*-dimethyl groups on the central carbon of one or both trimethylene bridges in [14]ane S_4 (to generate Me_2 -[14]ane S_4 and Me_4 -[14]ane S_4 ; see Figure 1) resulted in a 7-fold increase in Ni^{II} complex stability per *gem*-dimethyl group. They attributed this stability enhancement to the steric influence of the *gem*-dimethyl groups in promoting an endo conformation, thereby reducing the unfavorable entropy associated with complexation.

More recently, Hay and Hancock¹⁰ have stressed the concept that constraints placed upon donor atom orientation within macrocyclic ligands can be more important than the

cavity size or endo–exo equilibria in terms of the overall effect upon metal complex stabilities. In pursuing this theme, they noted that “the possible orientations of two adjacent donor atoms are largely controlled by the structure linking them together.” Comba and Schiek¹¹ have specifically addressed the effect of constraining the ethylene-linked nitrogen donors in [14]ane N_4 (i.e., 1,4,8,11-tetraazacyclotetradecane or cyclam) by substituting additional bridging ethylene groups and have concluded that the resulting stresses built into the ligand backbone “lead to considerable distortion and strain.” However, no thermodynamic or kinetic data are available to substantiate their theoretical predictions.

In an earlier examination of the influence of linker substituents on the properties of macrocyclic tetrathiaether complexes, we conducted thermodynamic and kinetic measurements on a complete series of substituted derivatives of [14]ane S_4 (L0) in which one or both ethylene bridges were replaced by all possible combinations of *cis*- and *trans*-1,2-cyclohexane (L2, L3, and L7–L11; see Figure 1).^{12–15} The dicyclohexanediyl derivatives were specifically designed to maintain constant inductive and solvation effects so that any differences in thermodynamic and kinetic properties should reflect differences in the steric constraints imposed on the orientation of the donor atoms. The resulting Cu^{II} L stability constants were enhanced by 10 – 10^4 times relative to the unsubstituted parent ligand, [14]ane S_4 , to yield an overall macrocyclic effect of 10^3 – 10^6 . Thus, the constraining influence of substituent groups upon the preferred orientation of the donor atoms was clearly demonstrated.

In the current work, we have generated a related series of substituted macrocycles in which the ethylene bridges in [14]ane S_4 are systematically replaced by *cis*- and *trans*-1,2-cyclopentane to generate ligands L23–L29 (Figure 1). Cyclopentane is much less flexible than cyclohexane, suggesting that its incorporation into the macrocyclic ligand backbone should have a more profound effect upon the resultant metal complexes. This report describes (i) the ligand syntheses and characterization, (ii) determination of the Cu^{II} L stability constants, (iii) measurement of the Cu^{II} L formation and dissociation rate constants, (iv) determination of the Cu^{II} L redox potentials, (v) calculation of the Cu^{I} L stability constants, and (vi) determination of the crystal structures for (a) the Cu^{II} L perchlorate salts with all five dicyclopentanediy-derivatized ligands (L25–L29), (b) the Cu^{I} (L28) complex, and (c) the free ligand, L25. All studies were conducted in 80% methanol/20% water (by weight) to afford sufficient ligand solubility to facilitate these measurements.

(8) Desper, J. M.; Gellman, S. H. *J. Am. Chem. Soc.* **1990**, *112*, 6732–6734.

(9) Desper, J. M.; Gellman, S. H.; Wolf, R. E., Jr.; Cooper, S. R. *J. Am. Chem. Soc.* **1991**, *113*, 8663–8671.

(10) Hay, B. P.; Hancock, R. D. *Coord. Chem. Rev.* **2001**, *212*, 61–78.

(11) Comba, P.; Schiek, W. *Coord. Chem. Rev.* **2003**, *238–239*, 21–29.

(12) Aronne, L.; Dunn, B. C.; Vyvyan, J. R.; Souvignier, C. W.; Mayer, M. J.; Howard, T. A.; Salhi, C. A.; Goldie, S. N.; Ochrymowycz, L. A.; Rorabacher, D. B. *Inorg. Chem.* **1995**, *34*, 357–369.

(13) Aronne, L.; Yu, Q.; Ochrymowycz, L. A.; Rorabacher, D. B. *Inorg. Chem.* **1995**, *34*, 1844–1851.

(14) Salhi, C. A.; Yu, Q.; Heeg, M. J.; Villeneuve, N. M.; Juntunen, K. L.; Schroeder, R. R.; Ochrymowycz, L. A.; Rorabacher, D. B. *Inorg. Chem.* **1995**, *34*, 6053–6064.

(15) Yu, Q.; Salhi, C. A.; Ambundo, E. A.; Heeg, M. J.; Ochrymowycz, L. A.; Rorabacher, D. B. *J. Am. Chem. Soc.* **2001**, *123*, 5720–5729.

Experimental Section

General Approach to Ligand Syntheses. The synthetic procedures for preparing the monosubstituted cyclopentanediy ligands, designated as *cis*- and *trans*-cyp-[14]aneS₄ (L23 and L24), have been previously described, including the preparation of *cis*- and *trans*-1,2-cyclopentanedithiol as starting materials.¹⁶ The synthetic route utilized to generate the dicyclopentanediy ligands (L25–L29) was formally analogous to that described previously for the corresponding diphenylene and dicyclohexanediy derivatives¹² and involved (i) condensation of *cis*- or *trans*-1,2-cyclopentanedithiol with 2 equiv of 3-chloropropanol to afford the corresponding *cis*- or *trans*-1,2-bis[(3-hydroxypropyl)thio]cyclopentanes, (ii) conversion of the alcohol derivatives to the corresponding 1,2-bis[(3-chloropropyl)thio]cyclopentanes, and (iii) high-dilution cyclocondensation of the chloro derivatives with *cis*- or *trans*-1,2-cyclopentanedithiol. (As noted earlier, several attempts to prepare these ligands by the seemingly simpler design strategy of high-dilution cyclocondensation of the *cis*- or *trans*-1,2-cyclopentanedithiols with 1,10-dichloro-4,7-dithiadecane resulted overwhelmingly in intrachain cyclization to 7- and 11-membered di- and trithiamocyclic products.) Likewise, the general separation and characterization techniques utilized for the various dicypt-[14]aneS₄ ligand stereoisomers were formally similar to those previously described for the corresponding dicyclohexane analogues.¹² Optimized isolation and purification procedures for the dicypt-[14]aneS₄ isomers are provided in detail in the following paragraphs. The identities of all cyclopentanediy-substituted ligands were eventually confirmed by X-ray crystallography because ¹³C NMR does not afford unequivocal distinction among the stereoisomers. Final products were determined to be analytically pure by gas chromatography–mass spectrometry (GC–MS), and elemental analysis.

Separation of a Diastereomeric Mixture of *syn*-2,3,9,10-*cis*,-*cis*-Dicyclopentano-1,4,8,11-tetrathiacyclotetradecane (*syn*-*cis*,-*cis*-dicypt-[14]aneS₄ = L25) and *anti*-2,3,9,10-*cis*,-*cis*-Dicyclopentano-1,4,8,11-tetrathiacyclotetradecane (*anti*-*cis*,-*cis*-dicypt-[14]aneS₄ = L26). The washed residue, 4.50 g, from 0.013-mol-scale condensation of *cis*-1,2-bis[(3-chloropropyl)thio]cyclopentane and *cis*-1,2-cyclopentanedithiol showed two nearly resolvable major thin-layer chromatography (TLC) components at *R*_f = 0.53 (isomer 1) and *R*_f = 0.45 (isomer 2) with 50:50 hexane/methylene chloride. Flash chromatography on a 2.5 × 40 cm silica gel column with 10:90 ethyl acetate/cyclohexane afforded a combined 1.65-g mixture fraction of the two isomers separated from a highly mobile forerun and column-bound higher polymers. Resolution of the isomers was achieved by careful elution chromatography on a 2.5 × 60 cm silica gel column with 90:10 hexane/methylene chloride. Two consecutive column runs were required to harvest substantially pure crops of 0.82 g of isomer 1 and 0.65 g of isomer 2. Recrystallization of isomer 1 (L26) from 15:85 ethyl acetate/hexane yielded colorless crystals. Mp: 150–151 °C, 0.71 g (16%). HRMS: calcd for C₁₆H₂₈S₄, 348.10739; found, 348.10771 (M⁺). EIMS: 348 (17), 174 (11), 173 (14), 107 (13), 106 (100), 67 (33). FT-IR (KBr, ν in cm⁻¹, relative intensity): 2951 (s), 2932 (s), 2914 (s), 2850 (s), 1446 (m), 1297 (m), 1249 (m), 1249 (m).

Recrystallization of isomer 2 (L25) from 5:95 methylene chloride/cyclohexane yielded colorless crystals. Mp: 139–141 °C, 0.49 g (11%). HRMS: calcd for C₁₆H₂₈S₄, 348.10739; 348.10734 (M⁺). EIMS: 348 (8), 137 (11), 107 (11), 106 (100), 95 (10), 81 (35), 73 (14), 69 (72), 67 (39), 57 (12), 55 (18). FT-IR (KBr, ν in cm⁻¹,

relative intensity): 2964 (s), 2944 (s), 2909 (s), 2862 (s), 1714 (w), 1442 (m), 1415 (m), 1309 (w), 1290 (m), 1216 (w), 1179 (w), 1128 (w), 1049 (w), 953 (w), 889 (w), 843 (w), 776 (w), 755 (w), 741 (w). During each recrystallization, traces of the alternate isomer were removed from the major isomer by treatment of the boiling recrystallization solution with approximately 0.05 g of charcoal (Darco-G-60) per 50 mL of solvent and hot gravity filtration.

Separation of a Diastereomeric Mixture of *meso*-2,3,9,10-*trans*,-*trans*-Dicyclopentano-1,4,8,11-tetrathiacyclotetradecane (*meso*-*trans*,-*trans*-dicypt-[14]aneS₄ = L27) and (*d,l*)-2,3,9,10-*trans*,-*trans*-Dicyclopentano-1,4,8,11-tetracyclotetradecane (*dl*-*trans*,-*trans*-[14]aneS₄ = L28). The washed residue, 7.25 g, from 0.021-mol-scale condensation of *trans*-1,2-bis[(3-chloropropyl)thio]cyclopentane and *trans*-1,2-cyclopentanedithiol showed the major product as an unresolvable band by TLC analysis at *R*_f = 0.50–0.55 with 10:90 ethyl acetate/hexane. Flash chromatography as for the *cis*,-*cis*-isomer ligands (L25 and L26) with 15:85 ethyl acetate/cyclohexane afforded 2.63 g of the diastereoisomeric mixture from other condensation products. Neither TLC nor elution column chromatography could resolve the isomers in our hands. However, repeated fractional recrystallization was tedious but effective. Repeated recrystallization from hexane afforded several crops of the *meso* isomer as determined by GC–MS analysis. Trace contaminants of the *d,l* isomer were removed by charcoal treatment, and final recrystallization from 20:80 cyclohexane/hexane afforded 0.96 g (13%) of colorless crystals (L27). Mp: 119–120 °C. HRMS: calcd for C₁₆H₂₈S₄, 348.10739; found, 348.10699 (M⁺). EIMS: 348 (12), 173 (13), 108 (10), 107 (28), 106 (100), 73 (14), 69 (16), 67 (33), 57 (11), 55 (13). FT-IR (KBr, ν in cm⁻¹; relative intensity): 2940 (s), 2916 (s), 2849 (s), 1440 (s), 1417 (m), 1296 (m), 1246 (m), 1181 (m).

The supernates from the recrystallization isolation of the *meso* isomer were recrystallized four times with charcoal treatment from 20:80 hexane/pentane and afforded 0.88 g (12%) of colorless crystals of the *d,l* isomers (L28). Mp: 83–84 °C. HRMS: calcd for C₁₆H₂₈S₄, 348.10739; found, 348.10715 (M⁺). EIMS: 348 (13), 173 (14), 108 (10), 107 (31), 106 (100), 73 (17), 69 (22), 67 (34), 60 (10), 57 (13), 55 (15). FT-IR (KBr, ν in cm⁻¹, relative intensity): 2950 (s), 1858 (m), 1441 (s), 1417 (m), 1296 (m), 1240 (s), 1185 (s), 833 (m), 693 (m).

Isolation of (*d,l*)-2,3-*cis*-9,10-*trans*-Dicyclopentano-1,4,8,11-tetrathiacyclotetradecane (*cis*,-*trans*-dicypt-[14]aneS₄ = L29). The washed residue, 3.80 g, from 0.011-mol-scale condensation of *trans*-1,2-bis[(3-chloropropyl)thio]cyclopentane and *cis*-1,2-cyclopentanedithiol showed the major condensation product at *R*_f = 0.55 by TLC analysis with 10:90 ethyl acetate/hexane. (Note: Attempted condensation of the alternative geometric isomer synthons likewise produced the desired ligand but in inferior yield.) Flash chromatography on a 2.5 × 55 cm silica gel column with 10:90 toluene/cyclohexane afforded the major product as a low-melting solid free of other reaction components. After three recrystallizations from 50:50 hexane/pentane with charcoal treatment at each step, 0.73 g (19%) of constant-melting, colorless crystals was isolated (L29). Mp: 82–83 °C. HRMS: calcd for C₁₆H₂₈S₄, 348.10739; found, 348.10725 (M⁺). EIMS: 348 (10), 173 (13), 107 (16), 106 (100), 81 (15), 73 (12), 69 (31), 67 (39), 55 (11). FT-IR (KBr, ν in cm⁻¹, relative intensity): 2945 (s), 2914 (s), 2861 (m), 1463 (w), 1441 (s), 1417 (m), 1295 (w), 1244 (s), 1211 (w), 1185 (w), 886 (w), 835 (w), 776 (w), 693 (w). [Note: Both electron-impact MS and ESMS revealed the presence of a significant amount of a compound with mass 480.1125 corresponding to C₂₁H₃₆S₆ (mass 480.1141), which represents an additional cyclopentanedithiolate moiety. The sharp melting point of the product combined with NMR analyses

(16) Wijetunge, P.; Kulatilake, C. P.; Dressel, C. P.; Dressel, L. T.; Heeg, M. J.; Ochrymowycz, L. A.; Rorabacher, D. B. *Inorg. Chem.* **2000**, *39*, 2897–2905.

demonstrated that this compound was not present in the initial purified sample and, therefore, must be a degradation product.]

Other Reagents. Copper(II) and mercury(II) perchlorate salts and subsequent solutions of these metal salts and of the ligands were prepared and standardized as previously described.¹² (**Warning!** All metal perchlorate salts are potentially explosive and should be handled with extreme care. These compounds should be prepared in small quantities and should never be dried.) All water utilized was distilled and then deionized and was of conductivity grade. Reagent-grade methanol was obtained from EM Science (Gibbstown, NJ) and used without further purification. Reagent-grade 70% perchloric acid was obtained from GFS Chemicals, Columbus, OH. The solvent utilized throughout this work was 80% methanol/20% water (by weight). The water content of all reagents (such as 70% perchloric acid) was taken into account when preparing solutions in this solvent mixture.

Instrumentation. All ultraviolet and visible spectra were obtained using a Hewlett-Packard 8452A diode array spectrophotometer. Quantitative absorbance measurements for stability constant determinations were made using a Cary model 17D dual-beam recording spectrophotometer equipped with a thermostated cell holder. All kinetic measurements were made using a Durrum D-110 stopped-flow spectrophotometer with a modified mixing system (Tritech, Winnipeg, Manitoba, Canada) that was interfaced to a PC. Constant ionic strength and perchlorate concentration were maintained by adding 0.10 M HClO₄. The temperature was controlled at 25.0 ± 0.2 °C using a constant-temperature water bath that provided circulation around the cell block and syringes. Reactions were monitored using the large S-to-Cu charge-transfer peak exhibited by the Cu^{II}L complexes in the region of 382–390 nm. Cyclic voltammograms (CVs) of Cu^{II}L were obtained using a BAS 100 electrochemical work station (Bioanalytical Systems, Lafayette, IN) operated at ambient temperature. A three-electrode electrochemical cell was used and consisted of a 3-mm glassy carbon disk working electrode, a Pt wire auxiliary electrode, and a Ag/AgCl (3 M NaCl) reference electrode (from Bioanalytical Systems), with the last electrode having a measured aqueous potential of 0.226 V vs SHE (as contrasted to the supplier's published potential value of 0.208 V).¹⁷

Crystal Structures. Crystals of the Cu^{II} complexes formed with the five dicyclopentanediyil derivatives of 1,4,8,11-tetrathiacyclotetradecane (L25–L29) were grown by slow evaporation from acetonitrile (L25), methanol/water mixtures (L26–L28), or acetonitrile/water mixtures (L29) containing essentially stoichiometric amounts of Cu(ClO₄)₂ and ligand. The crystal of Cu^I(L28) was grown by evaporation from an acetonitrile solution containing Cu(CH₃CN)₄ClO₄ and ligand under a nitrogen atmosphere. All diffraction data were collected at room temperature on a Bruker P4/CCD diffractometer equipped with Mo K α radiation. For each collection, 1650 frames were collected at 10 s frame⁻¹ with 0.3° between each frame. The frame data were integrated with the manufacturer's SMART and SAINT software. Absorption corrections were applied with Sheldrick's SADABS program, and the structure was solved and refined using the programs of SHELX-93 and SHELX-97. All non-hydrogen atoms were refined anisotropically.

(i) [Cu^{II}(L25)(ClO₄)₂]. The complex crystallized as dark purple irregular fragments. Hydrogen atoms were placed at observed positions and refined. The two independent perchlorate anions are

both bound in axial sites to the copper atom through oxygen. Typically, large thermal parameters are exhibited by the perchlorate oxygen atoms.

(ii) [Cu^{II}(L26)(ClO₄)₂]. The complex crystallized as dark tablets. The copper atom occupies a crystallographic inversion center and is bound to perchlorate oxygen atoms in the axial positions. Hydrogen atoms were placed in observed positions and refined.

(iii) [Cu^{II}(L27)(ClO₄)₂]. The complex crystallized as dark hexagonal drums. The copper occupies a crystallographic inversion center and is bound to equivalent perchlorate oxygen atoms in the axial positions. Hydrogen atoms were placed in observed positions and refined.

(iv) [Cu^{II}(L28)(H₂O)(ClO₄)₂]. The complex crystallized as dark green plates. The five-coordinate copper center is bound to the four sulfur atoms of the ligand and one axial water molecule. The perchlorate oxygen atoms are separated from the Cu by more than 4 Å. The asymmetric unit contains half of the complex and one independent perchlorate anion. Cu1 and O1 occupy a crystallographic 2-fold rotation axis. The hydrogen atoms were placed in calculated positions except for the hydrogen atoms on the coordinated water, which were observed.

(v) [Cu^{II}(L29)(ClO₄)ClO₄]. The complex crystallized as the diperchlorate salt in purple plates. One of the perchlorate anions is bound at the axial site to the copper atom through oxygen; another perchlorate is remotely located. One of the cyclopentane substituents assumed two conformations and was described using partial-occupancy carbon atoms: C9, C10, and C13 each were assigned two positions at 0.5 occupancy. Hydrogen atoms were placed in observed positions and refined isotropically, except for one hydrogen in the disorder region, which was placed in a calculated position. All atoms occupy general positions in the unit cell.

(vi) [Cu^I(L28)ClO₄]. This reduced complex crystallized as colorless multifaceted crystals. The asymmetric unit contains two cations and two perchlorate anions. The copper atoms are bound to the four sulfur atoms of the macrocycle; no perchlorate oxygen atom is closer than 4 Å from the copper atom. The hydrogen atoms were placed in calculated positions.

(vii) L25. The neutral ligand crystallized as colorless thin needles. Hydrogen atoms were placed in calculated positions and held riding their carbons. All atoms occupy general positions in the unit cell.

Results

Determination of Cu^{II} Complex Stability Constants.

Previous studies have shown that the perchlorate anion (as well as other "noncomplexing" anions) appears to form an adduct with copper(II) macrocyclic tetrathiaether complexes, which results in an apparent enhancement in the overall stability constants.^{18–20} Therefore, the perchlorate ion concentration was maintained at a constant level of 0.10 M for all equilibrium measurements. The conditional stability constant for each Cu^{II} complex is then defined by the relationship

(18) Young, I. R.; Ochrymowycz, L. A.; Rorabacher, D. B. *Inorg. Chem.* **1986**, *25*, 2576–2582.

(19) Nazarenko, A. Y.; Izatt, R. M.; Lamb, J. D.; Desper, J. M.; Matysik, B. E.; Gellman, S. H. *Inorg. Chem.* **1992**, *31*, 3990–3993.

(20) Diaddario, L. L., Jr.; Ochrymowycz, L. A.; Rorabacher, D. B. *Inorg. Chem.* **1992**, *31*, 2347–2353. In addition to perchlorate adducts, this study showed that the copper(II) tetrathiaether macrocyclic complexes also formed adducts with other potentially noncomplexing anions such as tetrafluoroborate and trifluoromethylsulfonate (triflate).

(17) Ambundo, E. A.; Deydier, M.-V.; Grall, A. J.; Aguera-Vega, N.; Dressel, L. T.; Cooper, T. H.; Heeg, M. J.; Ochrymowycz, L. A.; Rorabacher, D. B. *Inorg. Chem.* **1999**, *38*, 4233–4242. For notes on the potential of the Ag/AgCl electrode, see footnote 66.



$$K_{\text{Cu}^{\text{II}'}\text{L}'} = [\text{Cu}^{\text{II}'}\text{L}']/[\text{Cu}^{\text{II}'}][\text{L}] \quad (2)$$

$$K_{\text{Cu}^{\text{II}'}\text{L}'} = \frac{[\text{Cu}^{\text{II}'}\text{L}']}{(C_{\text{Cu}^{\text{II}}} - [\text{Cu}^{\text{II}'}\text{L}'])(C_{\text{L}} - [\text{Cu}^{\text{II}'}\text{L}'])} \quad (2a)$$

where L represents the uncomplexed ligand, C_{L} and $C_{\text{Cu}^{\text{II}}}$ represent the total concentrations of the ligand and Cu^{II} ion in solution, respectively, and the primed quantities include both the solvated species and any perchlorate adducts of Cu^{II} and the $\text{Cu}^{\text{II}'}\text{L}'$ complex.

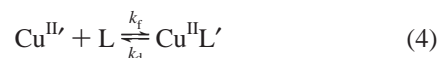
All of the copper(II) thiaether complexes included in the current study exhibit strong S-to-Cu charge-transfer bands in the vicinity of 390 nm, which facilitate the monitoring of the $\text{Cu}^{\text{II}'}\text{L}'$ concentration. For complexes with sufficiently large stability constants, it was assumed that the complexes were fully formed in the presence of a large excess of Cu^{II} , thereby permitting the value of the complex molar absorptivity, $\epsilon_{\text{Cu}^{\text{II}'}\text{L}'}$, to be determined independently. The concentration of $\text{Cu}^{\text{II}'}\text{L}'$ formed in solutions containing smaller amounts of the total Cu^{II} could then be calculated from the spectrophotometric absorbance and used to calculate the value of $K_{\text{Cu}^{\text{II}'}\text{L}'}$ by means of eq 2a. Because several of the Cu^{II} complexes included in this study were quite weak, however, it was often impossible to determine the value of $\epsilon_{\text{Cu}^{\text{II}'}\text{L}'}$ independently because solutions of known $\text{Cu}^{\text{II}'}\text{L}'$ concentration could not be readily prepared. In such cases, the McConnell–Davidson method was utilized, in which the $\epsilon_{\text{Cu}^{\text{II}'}\text{L}'}$ and $K_{\text{Cu}^{\text{II}'}\text{L}'}$ values were determined simultaneously.²¹ In this approach, a series of solutions were prepared and contained a constant amount of ligand and increasing amounts of excess Cu^{II} ion. The absorbance data were then plotted according to eq 3, in which

$$\frac{bC_{\text{L}}}{A} = \frac{1}{\epsilon_{\text{Cu}^{\text{II}'}\text{L}'}} + \frac{1}{\epsilon_{\text{Cu}^{\text{II}'}\text{L}'}K_{\text{Cu}^{\text{II}'}\text{L}'}(C_{\text{Cu}^{\text{II}}} - [\text{Cu}^{\text{II}'}\text{L}'])} \quad (3)$$

b represents the path length of the spectrophotometric cell (in cm) and A represents the measured absorbance. The $[\text{Cu}^{\text{II}'}\text{L}']$ term in the denominator was initially ignored, and subsequent corrections were made by iteration. The resulting molar absorptivity and stability constant values for all seven complexes included in this work are listed in Table 1, along with the corresponding values for the parent complex.

For all systems, attempts were made to determine the value of $K_{\text{Cu}^{\text{II}'}\text{L}'}$ using both eqs 2a and 3. Because significant differences were obtained using these approaches in some cases, an independent analysis of the stabilities was attempted based on the determination of the complex formation and dissociation kinetics as described below.

Complexation Kinetics. The rate constants for complex formation and dissociation, k_{f} and k_{d} , respectively, were studied under pseudo-first-order conditions by monitoring the increase



in absorbance at 390 nm following the mixing of a ligand solution with a large excess of Cu^{II} in a stopped-flow spectrophotometer. Because most of these reactions did not proceed to completion, the kinetics were treated in terms of the reversible differential expression

$$d[\text{Cu}^{\text{II}'}\text{L}']/dt = k_{\text{f}}[\text{Cu}^{\text{II}'}][\text{L}] - k_{\text{d}}[\text{Cu}^{\text{II}'}\text{L}'] \quad (5)$$

Under conditions in which no complex was initially present, the observed pseudo-first-order rate constant obtained can be represented as

$$k_{\text{obs}} = k_{\text{f}}[\text{Cu}^{\text{II}'}] + k_{\text{d}} \approx k_{\text{f}}C_{\text{Cu}^{\text{II}}} + k_{\text{d}} \quad (6)$$

Thus, a plot of k_{obs} vs $C_{\text{Cu}^{\text{II}}}$ should yield k_{f} as the slope and k_{d} as the intercept. In each case, the data were weighted by the reciprocal standard deviation, yielding the resolved values listed in Table 1.

For those reactions that proceeded nearly to completion, the intercepts were not statistically significant. Therefore, the dissociation rate constants were also determined independently by mixing ligand solutions containing a large excess of Cu^{II} with $\text{Hg}^{\text{II}}(\text{ClO}_4)_2$ solutions. The Hg^{II} ion forms complexes that are sufficiently strong to displace Cu^{II} either by scavenging the dissociated ligand or by forming an intermediate bimetallic complex. This results in two competing reaction pathways, as has been previously described.²⁰ For the current set of Cu^{II} complexes, both pathways were generally relevant so that the overall reaction kinetics conformed to eq 7, where k_{Hg} represents the formation rate

$$-d[\text{Cu}^{\text{II}'}\text{L}']/dt = k_{\text{d}}[\text{Cu}^{\text{II}'}\text{L}'] + k_{\text{Hg}}[\text{Hg}^{\text{II}}][\text{Cu}^{\text{II}'}\text{L}'] \quad (7)$$

constant for the bimetallic intermediate. Because the Hg^{II} concentration was in large excess over the total ligand, the reactions obeyed pseudo-first-order kinetics in which the apparent first-order rate constant, k_{app} , can be expressed as²⁰

$$k_{\text{app}} = k_{\text{d}} + k_{\text{Hg}}[\text{Hg}^{\text{II}}] \quad (8)$$

A plot of k_{app} vs $[\text{Hg}^{\text{II}}]$ yielded k_{d} as the intercept and k_{Hg} as the slope. The resolved rate constants obtained by this approach are included in Table 1.

The ratio of the Cu^{II} complex formation and dissociation rate constants should be identical with the overall stability constant because the reaction kinetics give no evidence for a buildup of intermediate species, that is

$$K_{\text{Cu}^{\text{II}'}\text{L}'} = k_{\text{f}}/k_{\text{d}} \quad (9)$$

The resultant stability constants obtained from the ratios of the k_{f} and k_{d} values are also listed in Table 1.

Redox Potentials. Slow-scan CVs were run at ambient temperature on solutions in 80% methanol containing approximately 10^{-3} M Cu^{II} and 10^{-5} M ligand for each of the cyclopentane-substituted ligands. The ionic strength was controlled at 0.10 M by adding 0.09 M NaNO_3 and 0.01 M HNO_3 . All potentials were referenced to ferrocene, for which

(21) McConnell, H.; Davidson, N. *J. Am. Chem. Soc.* **1950**, *72*, 3164–3167. Compare: Benesi, H. A.; Hildebrand, J. H. *J. Am. Chem. Soc.* **1949**, *71*, 2703–2707.

Table 1. Formation, Dissociation, and Mercury-Exchange Rate Constants and Conditional Stability Constants for the Cu^{II} Complexes Formed with the Cyclopentanediy Derivatives of [14]aneS₄ As Determined in 80% Methanol at 25.0 °C, $\mu = 0.10$ M (ClO₄⁻)^a

complexed ligand	$10^{-3}k_{\text{CuII}}, \text{M}^{-1} \text{cm}^{-1}$	$10^{-4}k_{\text{r}}, \text{M}^{-1} \text{s}^{-1}$	$k_{\text{d}}, \text{M}^{-1}$		$10^{-3}k_{\text{Hg}}, \text{M}^{-1} \text{s}^{-1}$	$10^{-4}K_{\text{CuII}}', \text{M}^{-1}$	
			form. kin.	Hg disp.		thermo ^c	kinetic ^d
L0	10.56(5) ^e	2.25(7) ^f	7.6(8) ^f	7(1) ^g	2.5(1) ^g	0.300(2) ^e	0.30(2) ^f
L23	6.2(4) [6.8]	2.23(3)	^h	1.50(9)	1.8(2)	1.4(2) [2.5]	1.5(4)
L24	6.7(8) [7.2]	0.55(4)	24(2)	22.5(8)	14(1)	0.0357(7) [0.030]	0.024(2)
L25	7.7(7) [6.6]	4.7(1)	^h	0.06(3)	0.29(8)	77(1)	77(4)
L26	4.61(7) [7.3]	1.40(3)	16.2(5)	10.5(3)	ⁱ	0.231(5) [0.20]	0.133(5)
L27	14(2) [9.8]	0.0036(1)	1.79(5)	1.55(4)	1.07(9)	0.00354(9)	0.0023(1)
L28	6.10(5) [5.5]	0.130(4)	73(6)	71(2)	12(4)	0.00272(3)	0.00183(8)
L29	^j [7.1]	0.89(2)	7(1)	6.7(6)	10(1)	^j [0.20]	0.13(1)

^a Values in parentheses in this and subsequent tables represent the standard deviations relative to the last digit shown; e.g., 2.25(7) represents 2.25 ± 0.07 .

^b The first values listed were determined from eq 3; the values in brackets were calculated from the absorbance of solutions containing a large excess of Cu^{II} based on the assumption that the complex was fully formed under these conditions; the latter values are presumed to be more accurate except for the weak complexes formed by L27 and L28, where the underlying assumption may not be valid. ^c The first values listed were determined from eq 3; the values in brackets were determined from eq 2a. ^d Calculated as the ratio of $k_{\text{f}}/k_{\text{d}}$ (eq 9). ^e Reference 12. ^f Reference 13. ^g Determined in aqueous solution.²⁰ ^h The intercept based on eq 6 was not statistically significant. ⁱ The slope based on eq 8 was not significant. ^j The intercept based on eq 3 was not statistically significant.

Table 2. CV Data for the Cu^{II/I} Complexes Formed with Cyclopentanediy Derivatives of 1,4,8,11-Tetrathiacyclotetradecane in 80% Methanol (by weight) at Ambient Temperature, $\mu = 0.10$ M (0.09 M NaNO₃ and 0.01 M HNO₃)

complexed ligand	potential values vs ferrocene ^{a,b}			
	E_{pc}, mV	E_{pa}, mV	$E_{1/2}, \text{mV}$	$\log K_{\text{CuII}}', \text{c}$
solvent			-321 ^d	
L0 ([14]aneS ₄)	135	227	181	12.0
L23 (<i>cis</i> -cyp-[14]aneS ₄)	72	161	117	11.5
L24 (<i>trans</i> -cyp-[14]aneS ₄)	183	270	227	11.8
L25 (<i>syn-cis,cis</i> -dicypt-[14]aneS ₄)	36	112	74	12.6
L26 (<i>anti-cis,cis</i> -dicypt-[14]aneS ₄)	152	212	182	11.9
L27 (<i>meso-trans,trans</i> -dicypt-[14]aneS ₄)	136	193	164	9.7
L28 (<i>dl-trans,trans</i> -dicypt-[14]aneS ₄)	240	357	299	11.9
L29 (<i>cis,trans</i> -dicypt-[14]aneS ₄)	163	228	196	12.0

^a In this work, the $E_{1/2}$ potential for ferrocene was determined to be 307 mV vs a Ag/AgCl reference electrode; for the latter electrode, the potential has been found to be 226 mV vs SHE for measurements in aqueous solution (ref 17). ^b Mean of three replicate measurements using a scan rate of 20 mV s⁻¹. ^c Calculated using eq 9. ^d The value shown represents solvated Cu^{II/I} in 80% methanol: ref 12, Table 2.

a potential of 0.307 V was obtained versus a micro Ag/AgCl reference electrode. The mean values for the cathodic and anodic peak potentials (E_{pc} and E_{pa}) obtained at a scan rate of 20 mV s⁻¹ are listed in Table 2. All but one of the complexes showed reasonable reversibility, with ΔE_{p} values ranging from 57 to 92 mV, the lone exception being the L28 system, for which $\Delta E_{\text{p}} = 117$ mV. The resulting half-wave potentials, $E_{1/2}$, are included in Table 2. Also included in this table is the potential value for solvated Cu^{II/I} in 80% methanol as previously determined.¹²

Cu^I Complex Stability Constants. The stability constants for the Cu^IL complexes in 80% methanol can be calculated directly from the Nernst equation using the redox potentials listed in Table 2:

$$E_{\text{CuII/L}}^{\text{f}} = E_{\text{CuII/soIV}}^{\text{f}} - \frac{2.303RT}{\mathcal{F}} \log \frac{K_{\text{CuII}}'}{K_{\text{CuI}}} \quad (10)$$

In eq 10, $E_{\text{CuII/L}}^{\text{f}}$ represents the formal potential of the Cu^{II/I}L complex (assumed to be identical with the $E_{1/2}$ values), $E_{\text{CuII/soIV}}^{\text{f}}$ is the formal potential of the solvated Cu^{II/I} redox

couple in 80% methanol,¹² and K_{CuI}' is the conditional stability constant for the reduced complex defined as

$$K_{\text{CuI}}' = [\text{Cu}^{\text{I}}\text{L}']/[\text{Cu}^{\text{I}}][\text{L}] \quad (11)$$

where the primed quantities include any anion complexes that may form in 0.10 M ClO₄⁻. As shown in Table 2, all but one of the resultant K_{CuI}' values are relatively uniform at around 10¹². As we have previously shown, the stability constants for a wide range of Cu^IL complexes with macrocyclic, acyclic, and tripodal ligands containing sulfur and/or saturated or unsaturated nitrogen donor atoms tend to exhibit logarithmic K_{CuI}' values of 13 ± 2 .^{17,22} Interestingly, a comparison of the Cu^IL stability constants with the previously studied cyhx-substituted ligands reveals that the current series of complexes with the cyp-substituted ligands are approximately 100-fold *less* stable. This suggests that the decreased flexibility imparted by the fused cyclopentane rings makes it more difficult for the ligands to adapt to a tetrahedral environment. It is particularly noteworthy that the K_{CuI}' value for L27 is more than 100-fold smaller than those for all other complexes in this series. Molecular models confirm the conclusion that the preferential orientation of the donor atoms imposed by the two cyclopentane rings makes it difficult for this specific ligand to adopt the most favorable tetrahedral geometry in which the lone-pair electrons alternate direction as one moves around the macrocycle.²³

Structural Determinations. Crystal structures for the Cu^{II} complexes with the monocyclopentanediy derivatives of [14]aneS₄ (L23 and L24) have been previously reported.¹⁶ The crystal structures of the Cu^{II} complexes with the five dicyclopentanediy derivatives were resolved as part of the current investigation. We have also determined the crystal structures of the reduced complex formed with L28 and for the free ligand L25. The experimental parameters for all seven structures are listed in Table 3. The resolved structures are shown as ORTEP drawings in Figures 2–8. The bond

(22) Rorabacher, D. B. *Chem. Rev.* **2004**, *104*, 651–697, Figure 3.

(23) Villeneuve, N. M.; Schroeder, R. R.; Ochrymowycz, L. A.; Rorabacher, D. B. *Inorg. Chem.* **1997**, *36*, 4475–4483.

Table 3. Crystal Parameters and Experimental Data for X-ray Diffraction Measurements on the Cu^{II} Complexes Formed with All Five Dicyclopentanediy-[14]aneS₄ Ligands and with the Cu^I Complex of *dl-trans,trans*-Dicyclopentanediy-[14]aneS₄ (X = ClO₄)^a

param	[Cu ^{II} (L25)]X ₂	[Cu ^{II} (L26)]X ₂	[Cu ^{II} (L27)]X ₂	[Cu ^{II} (L28)(H ₂ O)]X ₂	[Cu ^{II} (L29)X]X	[Cu ^I (L28)]X	L25
emp. form.	CuC ₁₆ H ₂₈ S ₄ Cl ₂ O ₈	CuC ₁₆ H ₂₈ S ₄ Cl ₂ O ₈	CuC ₁₆ H ₂₈ S ₄ Cl ₂ O ₈	CuC ₁₆ H ₃₀ S ₄ Cl ₂ O ₉	CuC ₁₆ H ₂₈ S ₄ Cl ₂ O ₈	CuC ₁₆ H ₂₈ S ₄ ClO ₄	C ₁₆ H ₂₈ S ₄
fw	611.06	611.06	611.06	629.08	611.06	511.61	348.62
space group	<i>Pbca</i>	<i>P2₁/n</i>	<i>P2₁/c</i>	<i>Fdd2</i>	<i>P1</i>	<i>P1</i>	<i>P2₁/c</i>
<i>a</i> , Å	9.8065(6)	7.3272(9)	8.290(1)	14.490(2)	9.5588(9)	11.155(1)	8.3587(9)
<i>b</i> , Å	18.379(1)	8.6446(9)	14.142(2)	37.070(6)	11.056(1)	13.430(1)	21.919(3)
<i>c</i> , Å	26.479(2)	18.429(2)	10.096(2)	9.351(2)	11.858(1)	15.556(3)	10.056(1)
α, deg	90	90	90	90	93.821(2)	82.220(3)	90
β, deg	90	98.739(2)	90.404(3)	90	99.763(2)	83.460(2)	102.548(2)
γ, deg	90	90	90	90	107.376(2)	74.659(2)	90
<i>V</i> , Å ³	4772.5(5)	1153.8(2)	1183.5(3)	5022.8(13)	1169.5(2)	2219.5(5)	1798.4(3)
<i>Z</i>	8	2	2	8	2	4	4
<i>T</i> , K	295(2)	295(2)	295(2)	295(2)	295(2)	295(2)	295(2)
ρ_{calcd} , g cm ⁻³	1.701	1.759	1.715	1.664	1.735	1.531	1.288
μ , mm ⁻¹	1.530	1.582	1.542	1.459	1.561	1.499	0.518
<i>R</i> (<i>F</i>) ^b	0.0668	0.0257	0.0374	0.0364	0.0518	0.0550	0.0747
<i>R</i> _w (<i>F</i> ²) ^c	0.0979	0.0682	0.1130	0.0850	0.0964	0.1144	0.0953

^a $\lambda = 0.71703$ Å. ^b $R(F) = \sum ||F_o| - |F_c|| / \sum |F_o|$ for $2\sigma(I)$ reflections. ^c $R_w(F^2) = [\sum w(F_o^2 - F_c^2)^2 / \sum w(F_o^2)^2]^{1/2}$ for $2\sigma(I)$ reflections.

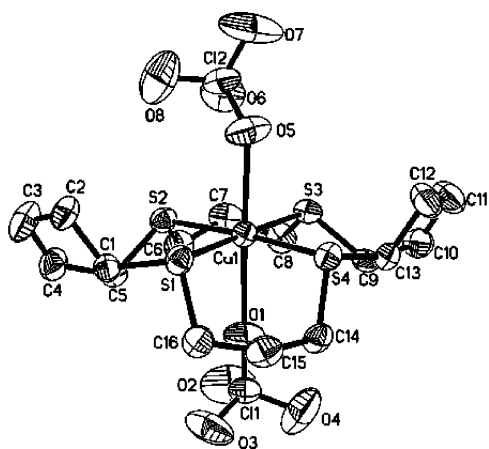


Figure 2. ORTEP drawing showing the structure of [Cu^{II}(L25)(ClO₄)₂]. Hydrogen atoms are omitted for clarity. The complex is in conformer I, although the copper is six-coordinate. The copper is nearly within the mean S₄ plane, although the Cu–O1 bond (to the perchlorate ion below the plane) is significantly longer than the Cu–O5 bond.

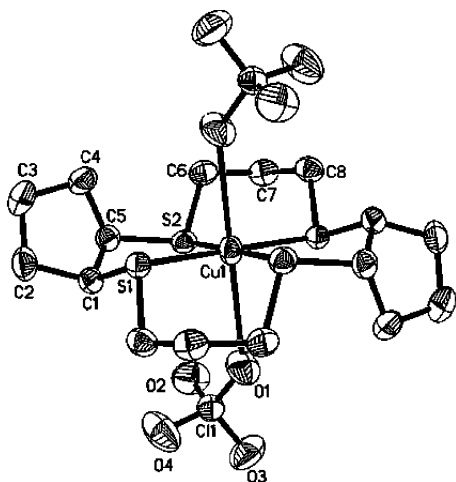


Figure 3. ORTEP drawing showing the structure of [Cu^{II}(L26)(ClO₄)₂]. Hydrogen atoms are omitted for clarity. The complex is in conformer III.

lengths and bond angles of primary interest for all six copper complex structures are compiled in Table 4.

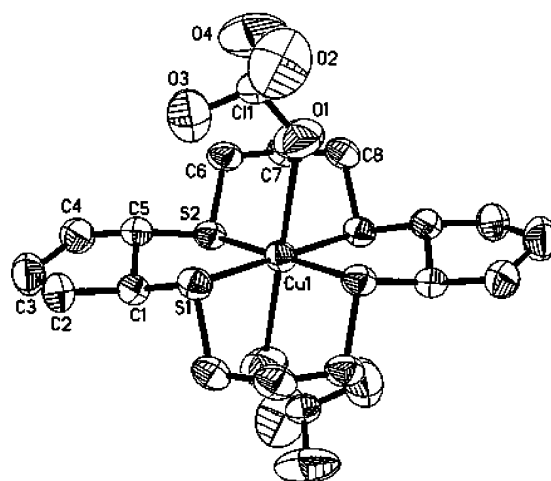


Figure 4. ORTEP drawing showing the structure of [Cu^{II}(L27)(ClO₄)₂]. Hydrogen atoms are omitted for clarity. The complex is in conformer III.

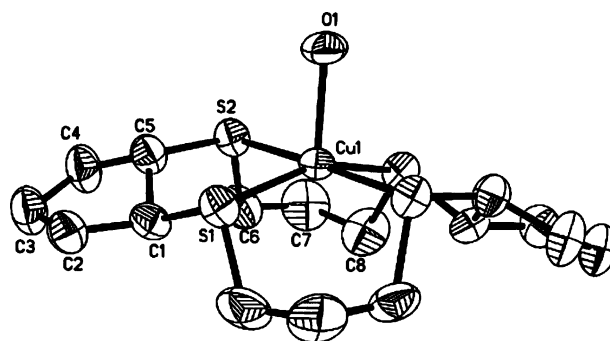


Figure 5. ORTEP drawing showing the structure of the cationic unit of [Cu^{II}(L28)(H₂O)](ClO₄)₂. Hydrogen atoms are omitted for clarity. The complex is in conformer I. The two *trans*-cyclopentane rings are canted in opposite directions so that the sulfur atoms are no longer coplanar. The copper atom is displaced out of the mean S₄ plane in the direction of the coordinated water molecule.

Discussion

Structural Considerations. Upon coordination by a metal ion, the donor atoms in [14]aneS₄ become chiral, resulting in five possible conformers, as defined earlier for the

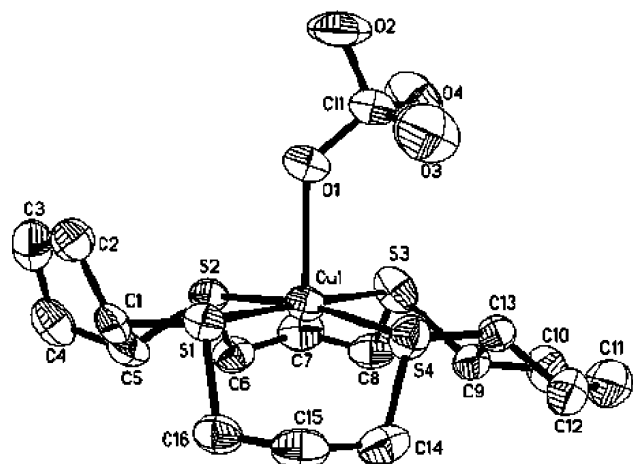


Figure 6. ORTEP drawing showing the structure of the cationic unit of $[\text{Cu}^{\text{II}}(\text{L29})(\text{ClO}_4)]\text{ClO}_4$. Hydrogen atoms are omitted for clarity. The complex is in conformer I. The copper atom is displaced very slightly out of the mean S_4 plane in the direction of the axially coordinated perchlorate.

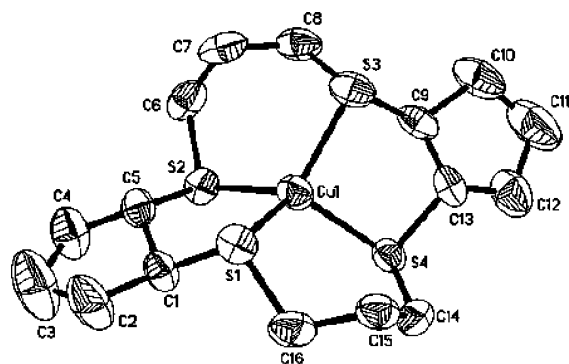


Figure 7. ORTEP drawing showing the structure of the cationic unit of $[\text{Cu}^{\text{II}}(\text{L28})]\text{ClO}_4$. Hydrogen atoms are omitted for clarity. The complex is in conformer V. The ligand is prevented from achieving a perfect tetrahedral coordination geometry by the constraints of the macrocyclic ring.

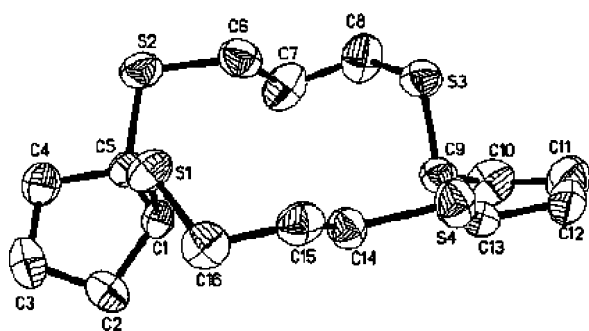


Figure 8. ORTEP drawing of the free L25 ligand. Hydrogen atoms are omitted for clarity. The lone pairs on all four sulfur donor atoms are oriented in the same direction relative to the "plane" of the macrocyclic ring, facilitating the coordination of a metal ion approaching from above.

corresponding complexes formed with the analogous tetraaza macrocycle, [14]ane N_4 (cyclam).²⁴ These five conformers are defined by the orientation of the amine hydrogens (in the tetraaza macrocycles) or the sulfur lone-pair electrons (in the tetrathia macrocycles) relative to the plane (or approximate plane) described by the four complexed donor atoms.²⁵ Of the five possible conformers, the $\text{Cu}^{\text{II}}\text{L}$ com-

plexes included in the current study tend to adopt either (i) conformer I, in which the lone-pair electrons on all four sulfur donor atoms are oriented on the same side of the S_4 plane (+ + + +), as shown for the complexes with L25, L28, and L29 in Figures 2, 5, and 6 [and also previously reported for $\text{Cu}^{\text{II}}(\text{L23})$ and $\text{Cu}^{\text{II}}(\text{L24})$],¹⁶ or (ii) conformer III, in which the pair of sulfur atoms bridged by one trimethylene bridge have their lone-pair electrons oriented toward the opposite side of the S_4 plane from the other pair of sulfurs (+ - - +), as shown in Figures 3 and 4 for the complexes with L26 and L27 (and also previously reported for the parent compound, $[\text{Cu}^{\text{II}}([\text{14}]\text{aneS}_4)(\text{ClO}_4)_2]$).²⁶

As shown in Table 5, identical conformations were previously observed in the crystal structures of the corresponding Ni^{II} and Cu^{II} complexes formed with the cyhx-[14]ane S_4 ligand series^{15,27} as well as the more limited examples of Ni^{II} complexes with cyhx-substituted [14]ane N_4 , with only three exceptions: (i and ii) $\text{Ni}^{\text{II}}(\text{trans-cyhx-[14]aneN}_4)$ and $\text{Ni}^{\text{II}}(\text{L11})$ adopted conformer III rather than conformer I, and (iii) $\text{Cu}^{\text{II}}(\text{L10})$ adopted the rarely observed conformer II, in which the lone-pair electrons on three of the coordinated sulfurs were oriented above the plane of the macrocyclic ligand while the fourth sulfur had its lone-pair electron oriented below the macrocyclic ligand plane (+ + + -).²⁸ In each series, the conformer observed for the parent complex and for the *anti-cis,cis*-derivatized complex is in agreement with the predictions for the $\text{Ni}^{\text{II}}([\text{14}]\text{aneN}_4)$ series as calculated by Donnelly and Zimmer²⁹ based on minimum strain (Table 5, column 2). However, the Ni^{II} and Cu^{II} complexes with the *meso-trans,trans-*, *dl-trans,trans-*, and *cis,trans*-dicyhx-[14]ane S_4 and the corresponding dicypt-substituted ligands generally differ from Donnelly and Zimmer's predictions. These apparent discrepancies presumably reflect the impact of the longer metal-sulfur bonds and alterations in the preferred Cu-S-C bond angles and Cu-S-C-C dihedral angles on internal ligand strain.^{10,30} This latter suggestion is supported by even comparatively elementary molecular mechanical calculations for the substituted [14]ane S_4 complexes (bracketed conformers in column 2 of Table 5), which largely agree with the conformers observed in the crystal structures of the Ni^{II} and Cu^{II}

(25) As noted in refs 12, 23, and 24, the five conformers are defined according to the orientations of the amine hydrogens or the sulfur lone-pair electrons relative to the donor atom plane as follows (where + represents above the plane, - is below the plane, and the order of the donor atoms is 1, 4, 8, and 11): conformer I, + + + +; conformer II, + + + -; conformer III, + - - +; conformer IV, + + - -; conformer V, + - + -.

(26) Glick, M. D.; Gavel, D. P.; Diaddario, L. L.; Rorabacher, D. B. *Inorg. Chem.* **1976**, *15*, 1190-1193.

(27) Kulatilleke, C. P.; Goldie, S. N.; Heeg, M. J.; Ochrymowycz, L. A.; Rorabacher, D. B. *Inorg. Chem.* **2000**, *39*, 1444-1453.

(28) The $\text{Cu}^{\text{II}}(\text{L10})$ complex is the only definitive example in the literature of a crystal structure for a divalent metal complex involving a quadridentate macrocyclic ligand for which the ligand is in conformer II. Conformer II has also been indicated for the blue form of copper(II) (*C-meso-5,5,7,12,12,14-hexamethyl-1,4,8,11-tetraazacyclotetradecane*), but the crystal structure was not satisfactorily resolved: Clay, R.; Murray-Rust, J.; Murray-Rust, P. *J. Chem. Soc., Dalton Trans.* **1979**, 1135-1139.

(29) Donnelly, M. A.; Zimmer, M. *Inorg. Chem.* **1999**, *38*, 1650-1658.

(30) DaCruz, M. F.; Zimmer, M. *Inorg. Chim. Acta* **1997**, *261*, 181-186.

Table 4. Comparison of Structural Parameters of Principal Interest in the Cationic Units of the Cu^{II} Complexes Formed with All Five Dicyclopentanediy-[14]aneS₄ Ligands and the Cu^I Complex with L28 (X = ClO₄)

	[Cu ^{II} (L25)]X ₂	[Cu ^{II} (L26)]X ₂	[Cu ^{II} (L27)]X ₂	[Cu ^{II} (L28)(H ₂ O)]X ₂	[Cu ^{II} (L29)X]X	[Cu ^I (L28)]X
conformer	I	III	III	I	I	V
			Bond Lengths, Å			
Cu–S1	2.325(1)	2.2722(5)	2.3181(7)	2.3137(9)	2.317(1)	2.295(2)
Cu–S2	2.290(1)	2.2887(4)	2.3094(7)	2.366(1)	2.288(1)	2.305(2)
Cu–S3	2.293(1)				2.322(2)	2.281(2)
Cu–S4	2.328(1)				2.333(1)	2.304(2)
Cu–O1	2.613(3)	2.759(2)	2.637(3)	2.142(5)	2.379(3)	
Cu–O5	2.461(4)					
			Bond Angles, deg			
S1–Cu–S2	87.53(5)	89.78(2)	91.72(2)	90.41(3)	88.66(5)	95.86(7)
S2–Cu–S3	96.77(5)	90.22(2)	88.28(2)	89.26(3)	91.75(5)	111.27(7)
S3–Cu–S4	87.87(5)				89.06(3)	96.07(7)
S4–Cu–S1	87.86(5)				89.17(4)	110.28(7)
S1–Cu–S3	175.64(5)	180.0	180.0	157.17(6)	178.49(5)	122.92(7)
S2–Cu–S4	174.71(5)			178.33(6)	169.96(4)	122.63(6)
S1–Cu–O1	95.48(9)	93.39(4)	92.87(7)	101.42(3)	90.30(9)	
S2–Cu–O1	84.72(9)	86.53(4)	101.35(8)	90.84(3)	93.68(9)	
S3–Cu–O1	85.62(9)				91.1(1)	
S4–Cu–O1	93.13(9)				96.0(1)	
S1–Cu–O5	88.6(1)					
S2–Cu–O5	94.5(1)					
S3–Cu–O5	90.4(1)					
S4–Cu–O5	88.0(1)					
O1–Cu1–O5	175.8(1)	180.0	180.0			
			Distortions from S ₄ Plane			
Cu displacement, ^a Å	–0.0181(8)	0	0	–0.2463(9)	–0.1120(8)	
S ₄ deviation, ^b Å	±0.0337	0	0	±0.0337	±0.0834	
dihedral angle, ^c deg			80.26(5)			

^a Cu atom displacement from the average S₄ plane (in Å). ^b Deviation of the sulfur donor atoms from the average S₄ plane. ^c Dihedral angle between the S1–Cu–S2 and S3–Cu–S4 planes (in deg).

Table 5. Conformers Found in Crystal Structures of Ni^{II} and Cu^{II} Complexes Formed with Cyclohexanediy (cyhx) and Cyclopentandiy (cypt)-Substituted Derivatives of [14]aneN₄ and [14]aneS₄

substituents	cyhx derivatives				cypt derivatives
	theor. min. energy	Ni ^{II} ([14]aneN ₄) ^a	Ni ^{II} ([14]aneS ₄) ^a	Cu ^{II} ([14]aneS ₄) ^b	Cu ^{II} ([14]aneS ₄) ^b
none	III, ^c I ^d	III ^{e,f}	III ^g	III ^h	III ^h
cis-	[I] ⁱ	I ^j		I ^k	I ^l
trans-	[I] ⁱ	III ^{j,m}		I ^k	I ^l
syn-cis,cis-	I, ^c [I] ⁱ	I ^m	I ⁿ	I ^o	I ^{p,q}
anti-cis,cis-	[III] ⁱ	III ^m	III ⁿ	III ^o	III ^p
meso-trans,trans-	I, ^c [III] ⁱ		III ⁿ	III ^o	III ^p
dl-trans,trans-	II, ^c [I] ⁱ		I ⁿ	II ^o	I ^p
cis,trans-	II, ^c [I] ⁱ		III ^{f,n}	I ^o	I ^p

^a All Ni^{II} complexes are low spin (four-coordinate square planar) except as noted. ^b All Cu^{II} complexes in conformer I are five-coordinate square pyramidal except as noted; all complexes in conformers II or III are six-coordinate tetragonal. ^c Minimum-energy conformers were calculated for the Ni^{II}([14]aneN₄) series.²⁹ ^d Adam, K. R.; Antolovich, M.; Brigden, L. G.; Lindoy, L. F. *J. Am. Chem. Soc.* **1991**, *113*, 3346–3351. Conformers I (low-spin square planar) and III (high-spin octahedral) appear to be close in energy for Ni^{II}([14]aneN₄) and NMR evidence indicates a rapid equilibration between the two conformers in solution: Connolly, P. J.; Billo, E. J. *Inorg. Chem.* **1987**, *26*, 3224–3226. ^e (i) Bosnich, B.; Mason, R.; Pauling, P. J.; Robertson, G. B.; Tobe, M. L. *J. Chem. Soc., Chem. Commun.* **1965**, 97–98. (ii) Prasad, L.; McAuley, A. *Acta Crystallogr.* **1983**, *C39*, 1175–1177. (iii) Thöm, V. J.; Fox, C. C.; Boeyens, J. C. A.; Hancock, R. D. *J. Am. Chem. Soc.* **1984**, *106*, 5947–5955. ^f Six-coordinate high-spin complex. ^g David, P. H.; White, L. K.; Belford, R. L. *Inorg. Chem.* **1975**, *14*, 1753–1757. ^h Reference 24. ⁱ Relative minimum-energy conformers in brackets were estimated with ChemBats3D Plus using the Cu^{II}(cycloalkyl-[14]aneS₄)Cl₂ series of complexes as models. ^j Reference 26. ^k Reference 14. ^l Reference 16. ^m Reference 27. ⁿ Reference 25. ^o Reference 15. ^p This work. ^q Six-coordinate tetragonal complex.

complexes with [14]aneS₄ derivatives, as noted in the last three columns of Table 5.³¹

In the structure of the lone reduced complex, Cu^I(L28) (Figure 7), the unshared lone-pair electrons on the sulfur donor atoms alternate as one proceeds around the macrocyclic ring to generate conformer V (+ – + –).²³ This same ligand conformation has been observed in all previous Cu^I complexes with macrocyclic tetrathiaethers having a ring size

(31) Our calculations are based on a minimization of the residual strain energies for Co^{II}LCl₂ (as a model complex) using Chem3D Plus. Although the overall energies are not reliable using this approach, the relative residuals should reflect the differences in the overall internal ligand strain in the various conformers because all other factors are reasonably equivalent for each conformer.

of 14 or larger.^{14–16,32} Therefore, this is presumed to represent the preferred conformation for all Cu^I complexes included in the current study.

Stability Constant Comparisons. Although there are some discrepancies between the stability constant values obtained from equilibrium measurements (eqs 2a and 3) and

(32) (a) Dockal, E. R.; Diaddario, L. L.; Glick, M. D.; Rorabacher, D. B. *J. Am. Chem. Soc.* **1977**, *99*, 4530–4532. (b) Corfield, P. W. R.; Ceccarelli, C.; Glick, M. D.; Moy, I. W.-Y.; Ochrymowycz, L. A.; Rorabacher, D. B. *J. Am. Chem. Soc.* **1985**, *107*, 2399–2404. (c) Bernardo, M. M.; Heeg, M. J.; Schroeder, R. R.; Ochrymowycz, L. A.; Rorabacher, D. B. *Inorg. Chem.* **1992**, *31*, 191–198. (d) Galijasevic, S.; Krylova, K.; Koenigbauer, M. J.; Jaeger, G. S.; Bushendorf, J. D.; Heeg, M. J.; Ochrymowycz, L. A.; Taschner, M. J.; Rorabacher, D. B. *Dalton Trans.* **2003**, 1577–1586.

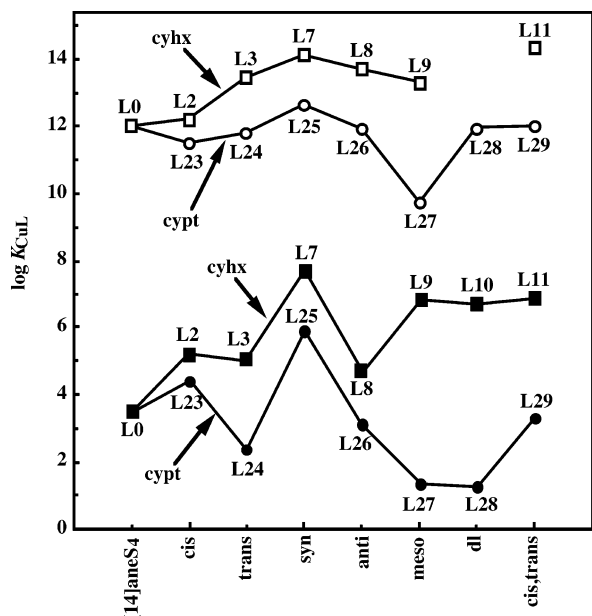


Figure 9. Logarithmic trends in copper complex stability constants in 80% methanol at 25 °C, $\mu = 0.10$ M (ClO_4^-). The solid symbols represent $\text{Cu}^{\text{II}}\text{L}$ values, and the open symbols represent $\text{Cu}^{\text{I}}\text{L}$ values. In both series, the square and circular symbols represent the cyclohexanediy- and cyclopentanediy-derivatized [14]aneS₄ ligands, respectively.

those obtained from the rate constant ratios (eq 9), as listed in the last two columns of Table 1, these differences are relatively insignificant compared to the overall trends. In this discussion, we refer principally to the equilibrium measurements because they tend to be more reliable. A comparison of the logarithmic stability constants for the $\text{Cu}^{\text{II}}\text{L}$ complexes with both the cyclopentane- and cyclohexane-substituted¹² series of [14]aneS₄ ligands (solid symbols in Figure 9) reveals that the $\text{Cu}^{\text{II}}\text{L}$ stability constants *increase* upon introduction of *cis*-cycloalkyl moieties, with the magnitude of the increase being approximately 10-fold for each *cis*-cypt group and approximately 30-fold for each *cis*-cyhx group. The lone exceptions to this trend are the *anti-cis,cis* diastereomers, which, in both series, are about 3 orders of magnitude less stable than their *syn-cis,cis* analogues. This contrasting behavior implies that the *anti* arrangement of *cis*-cycloalkyl substituents results in an unfavorable orientation of the four donor atoms.

Dramatically different trends are observed in the $\text{Cu}^{\text{II}}\text{L}$ stabilities for the two series of *trans*-cycloalkyl-substituted species. The introduction of each *trans*-cyhx ring results in an approximately 30-fold *increase* in the $\text{Cu}^{\text{II}}\text{L}$ stability, in parallel to the corresponding *cis*-cyhx derivatives. However, each *trans*-cypt substituent *decreases* the $\text{Cu}^{\text{II}}\text{L}$ stability by approximately 10-fold. As a result of this difference in behavior, the ligands containing two *trans*-cypt substituents (L27 and L28) are 10⁵ *less stable* than their *trans*-cyhx analogues (L9 and L10). Thus, it is apparent that the rigid *trans*-cyclopentane rings orient the adjacent donor atoms in such a way as to induce a large amount of internal strain when attempting to coordinate to Cu^{II} .

For the corresponding $\text{Cu}^{\text{I}}\text{L}$ complexes, the influence of the cypt and cyhx substituent groups upon the stability constants (open symbols in Figure 9) is somewhat less

dramatic because coordinate bond directionality is less significant in d¹⁰ systems. In general, the cypt-substituted ligands exhibit $\text{Cu}^{\text{I}}\text{L}$ stability constants that are within a factor of ± 3 of the parent complex, while the cyhx-substituted ligands are 20–200 times more stable. However, there is a notable deviation in the $\text{Cu}^{\text{I}}\text{L}$ stability with L27, which is 200 times *less* stable than the parent complex. This deviation is all the more remarkable in view of the fact that, for a huge number of uncharged multidentate ligands, we have previously shown that the logarithmic $K_{\text{Cu}^{\text{I}}\text{L}}$ values lie within the narrow range of 13 ± 2 regardless of ligand structure or donor atom type.^{17,22} The significant deviation in the Cu^{I} - (L27) stability implies that the steric constraints in this meso isomer prevent the donor atoms from twisting into a nonplanar array, as is normally found for four-coordinate $\text{Cu}^{\text{I}}\text{L}$ complexes.

There are few literature examples demonstrating the influence of cyclopentane substituents upon the stability of transition-metal complexes with macrocyclic ligands. The only relevant example appears to be that of Riley and co-workers, who showed that the replacement of one ethylene bridge in [15]aneN₅ by a *trans*-1,2-cyclopentane ring resulted in a 5-fold *decrease* in the stability of the Mn^{II} complex, whereas a *trans*-1,2-cyclohexane ring brought about a 6-fold *increase* in stability.³³ We note that these trends are in the same direction as those observed in the current study for mono-*trans*-cypt and -*trans*-cyhx derivatives, although the magnitude of these effects is smaller for the larger 15-membered macrocycle. (Interestingly, the study by Riley et al. also included the observation that incorporation of a single *trans*-1,2-cycloheptane ring had virtually no effect upon the stability, a result that is consistent with the greater flexibility of the 7-membered ring.³³)

Comparative Kinetic Behavior. According to eq 9, the large decrease in the stabilities of the $\text{Cu}^{\text{II}}\text{L}$ complexes formed with the *trans*-cypt-substituted ligands relative to the values for their *trans*-cyhx counterparts must reflect either a decrease in the formation rate constants or an increase in the dissociation rate constants or both. In our prior study on the cyhx-substituted ligand series,¹³ we observed that the k_f values for the complexation reactions with Cu^{II} were nearly uniform, all being within a factor of about 2 of the k_f value for the parent $\text{Cu}^{\text{II}}([\text{14}]\text{aneS}_4)$ complex. As illustrated in Figure 10, similar k_f values are observed for the *cis*-cypt-substituted ligands (L23 and L25), although the value for L26 was half that of its dicyhx analogue.¹³ By contrast, the ligands containing *trans*-cypt substituents (L24 and L27–L29) exhibit significantly smaller k_f values. In the most

(33) Riley, D. P.; Henke, S. L.; Lennon, P. J.; Weiss, R. H.; Neumann, W. L.; Rivers, W. J., Jr.; Aston, K. W.; Sample, K. R.; Rahman, H.; Ling, C.-S.; Shieh, J.-J.; Busch, D. H.; Szulbinski, W. *Inorg. Chem.* **1996**, *35*, 5213–5231. This same research group has also prepared Mn^{II} -([15]aneN₅) derivatives containing two fused *trans*-cyclohexane rings (i.e., *meso-trans,trans*-dicyhx-[15]aneN₅ and *dl-trans,trans*-dicyhx-[15]aneN₅), but no stability constant data have been reported: (a) Riley, D. P.; Lennon, P. J.; Neumann, W. L.; Weiss, R. H. *J. Am. Chem. Soc.* **1997**, *119*, 6522–6528. (b) Riley, D. P.; Henke, S. L.; Lennon, P. J.; Aston, K. *Inorg. Chem.* **1999**, *38*, 1908–1917. A related *dl-trans,trans*-dicyhx-substituted ligand has also been reported in which one amine nitrogen of [15]aneN₅ has been replaced by a pyridine nitrogen: Aston, K.; Rath, N.; Naik, A.; Slomczynska, U.; Schall, O. F.; Riley, D. P. *Inorg. Chem.* **2001**, *40*, 1779–1789.

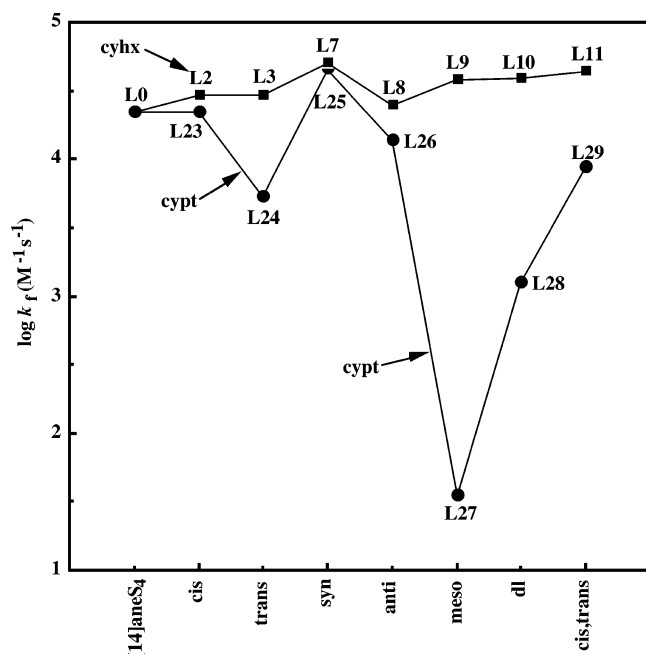


Figure 10. Logarithmic trends in $Cu^{II}L$ formation rate constants for reactions with the cyclohexanediyl- (squares) and cyclopentanediy-derivatized [14]ane S_4 ligands (circles) in 80% methanol at 25 °C, $\mu = 0.10$ M (ClO_4^-).

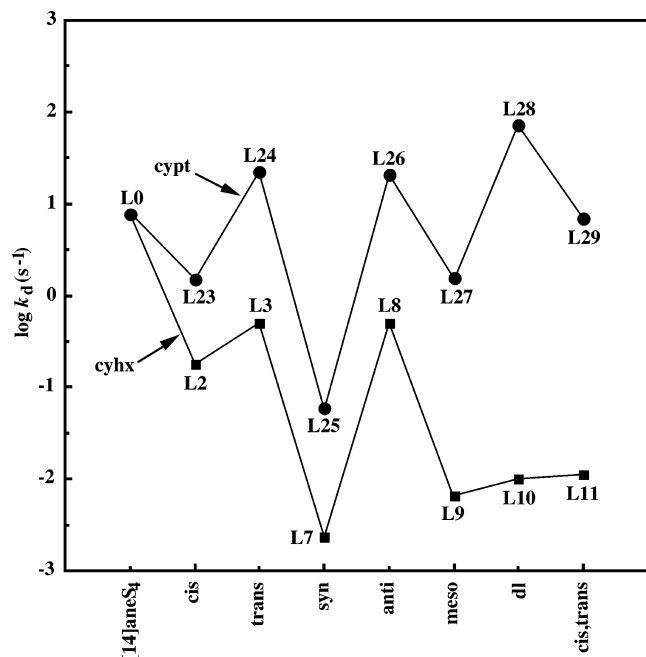


Figure 11. Logarithmic trends in $Cu^{II}L$ dissociation rate constants for complexes formed with the cyclohexanediyl- (squares) and cyclopentanediy-derivatized [14]ane S_4 ligands (circles) in 80% methanol at 25 °C, $\mu = 0.10$ M (ClO_4^-).

extreme case, the k_f value for the L27 complex is fully 3 orders of magnitude smaller than that for the corresponding dicyhx-substituted complex (L9).

A comparison of the dissociation rate constants for the two ligand series is provided in Figure 11. In all cases, the cypt-substituted complexes exhibit k_d values that are at least 10 times larger than their cyhx-substituted analogues, and even larger differences are apparent for the *trans,trans*-dicypt-substituted ligands. The L28 complex is particularly

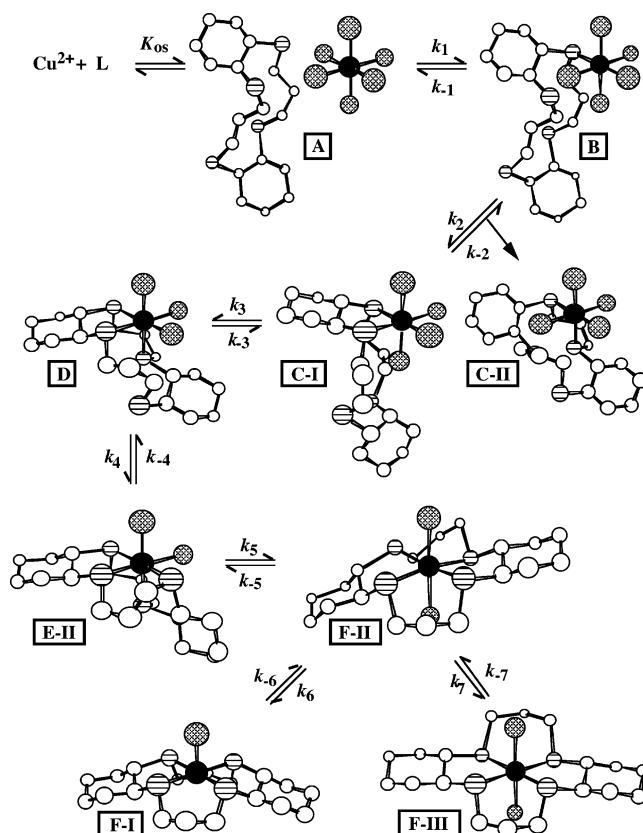


Figure 12. Schematic representation of the individual reaction steps in the formation and dissociation of Cu^{II} complexes with derivatized [14]ane S_4 ligands (from ref 13). The solid circle represents the copper atom, striped circles are sulfur atoms, cross-hatched circles are solvent molecules, and open circles are carbon atoms. (Hydrogen atoms have been omitted for clarity.)

notable in that its $Cu^{II}L$ complex dissociates nearly 10^4 times faster than the corresponding *dl-trans,trans*-dicyhx (L10) analogue.¹³

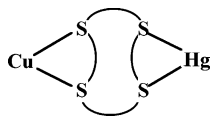
Stepwise Mechanistic Analysis for Complex Formation and Dissociation. The stepwise mechanism proposed previously^{13,27} for complex formation and dissociation involving Cu^{II} and macrocyclic tetrathiaether ligands is illustrated in Figure 12. In the *formation* process, previous studies have indicated that the closure of the first chelate ring to form intermediate C-I or C-II, as represented by rate constant k_2 , is the rate-determining step.^{13,34} This process requires the ligand to contort into a configuration that places a second donor atom close to the Cu ion prior to the rupture of a second Cu–solvent bond. The observation that the k_f values for most of the cyhx-substituted systems are slightly larger than for the parent [14]ane S_4 ligand (Figure 10) suggests that these cycloalkyl substituents tend to promote an endo conformation that facilitates the closure of the first chelate ring. Despite the promotion of a more nearly endo arrangement, the k_f values for the ligands containing *trans*-cypt moieties are significantly smaller, signifying that the two sulfur atoms attached to an uncomplexed *trans*-cyclopentane ring tend to orient their lone-pair electrons on opposite sides

(34) Diaddario, L. L.; Zimmer, L. L.; Jones, T. E.; Sokol, L. S. W. L.; Cruz, R. B.; Yee, E. L.; Ochrymowycz, L. A.; Rorabacher, D. B. *J. Am. Chem. Soc.* **1979**, *101*, 3511–3520.

of the macrocycle. Because of the reduced flexibility of the cyclopentane ring, this makes it difficult for the ligand to complete the first chelate ring. However, the observation that the *meso-trans,trans*-dicypt derivative reacts much more slowly than the *dl-trans,trans*-dicypt-substituted analogue is not readily explainable from an examination of molecular models.

As noted in the preceding section, the Cu^{II} dissociation rate constants for the majority of cypt-substituted ligands are 1–2 orders of magnitude larger than their cyhx counterparts and the increase in k_{d} values is even more marked for the *meso-trans,trans*-dicypt-, the *cis,trans*-dicypt-, and, especially, the *dl-trans,trans*-dicypt-derivatized ligands. In the proposed mechanism (Figure 12), the initial conformational changes in converting the final complex, F-I (conformer I) or F-III (conformer III), to the initial intermediates, F-II (conformer II) and E-II (a folded form of conformer II), have been previously considered by Canales and Zimmer for substituted [14]ane N_4 complexes and interpreted in terms of internal strain induced by peripheral substituents.³⁵ The more rapid dissociation of the complexes with the cypt-derivatized ligands compared to their cyhx counterparts suggests that these favor (i) the initial conformational changes (k_{-6}/k_6 or k_{-7}/k_7 and k_{-5}/k_5) and/or (ii) the equilibria involving first and/or second bond rupture (k_{-3}/k_3 and k_{-4}/k_4) due to increased strain. In this regard, it is interesting to note that $\text{Cu}^{\text{II}}(\text{L28})$, which exhibits the largest k_{d} value, is the only complex in this study that involves an S1–Cu–S3 bond angle that is significantly bent (Table 4). Thus, this species may more readily fold to generate intermediate E-II.

Some idea of the relative magnitude of the equilibria preceding the rate-determining step in the dissociation process may be obtained by comparing the k_{Hg} values for the displacement of Cu^{II} by Hg^{II} . This mechanism must involve the formation of a binuclear intermediate species in which Cu^{II} still maintains one chelate ring and Hg^{II} is also coordinated to one or, more likely, two donor atoms.²⁰ Because it is likely that two $\text{Cu}^{\text{II}}\text{--S}$ bonds must rupture before a binuclear intermediate can form to a significant extent, the magnitude of the k_{Hg} values should include the



product of $K_{-3}K_{-4}K_{-5}K_{-6}$ (or $K_{-3}K_{-4}K_{-5}K_{-7}$) in the complexation mechanism. Because the same terms contribute to the unaided complex dissociation rate constant (k_{d}), the $k_{\text{d}}/k_{\text{Hg}}$ ratio might be expected to be relatively uniform. In fact,

within each ligand series, this ratio is constant to within about a factor of 10. However, the $k_{\text{d}}/k_{\text{Hg}}$ ratios are uniformly 15–60 times larger for the cyhx series than for the cypt series (see Table S-15 in the Supporting Information), reflecting the fact that the replacement of cyhx substituents by cypt substituents results in a greater increase in k_{Hg} values than in k_{d} values. Thus, relative to the unaided complex dissociation process, Hg^{II} is significantly more effective in promoting the dissociation of the cypt series of ligands, an effect that is not readily explainable based on the present data.

As noted earlier, the Cu^{II} complex with the *syn-cis,cis*-dicypt-[14]ane S_4 ligand exhibits the largest formation rate constant and the smallest dissociation rate constant (as well as the smallest Hg^{II} exchange rate constant) of the current series. This behavior can be understood from the crystal structure of the free ligand (Figure 8), which shows that the lone-pair electrons for all four sulfur atoms tend to be oriented toward the same side of the macrocyclic ring. Thus, this ligand is poised to initiate complex formation and appears to undergo minimal internal ligand strain when fully complexed.

Conclusions. This study represents the first in which 1,2-cyclopentane groups have been systematically substituted for both ethylene bridges in a 14-membered quadridentate macrocyclic ligand, specifically [14]ane S_4 . Relative to the properties of corresponding 1,2-cyclohexane-substituted ligands, the greater rigidity of the cyclopentane rings is manifested in a general decrease in the stability constants for both the Cu^{II} and Cu^{I} complexes, with the maximum decrease being observed for the complexes involving the two *trans,trans*-dicypt diastereomers. From a kinetic standpoint, the *trans*-substituted ligands exhibited both smaller $\text{Cu}^{\text{II}}\text{L}$ formation rate constants and large increases in the dissociation rate constants, both factors contributing to the decreased stability. Both the thermodynamic and kinetic differences in the behavior of the substituted [14]ane S_4 complexes point to the greater importance of macrocyclic substituents in influencing donor atom orientation, as emphasized by Hay and Hancock,¹⁰ rather than merely serving to influence exo–endo equilibria.

Acknowledgment. This work was supported by the National Science Foundation under Grant CHE-0211696. The authors are indebted to Dr. Lew Hryhorczuk of Wayne State University's Central Instrument Facility for the mass spectral analyses of the ligand samples.

Supporting Information Available: Tables of kinetic data for the Cu^{II} complex formation reactions and Hg^{II} displacement reactions (Tables S-1–S-15). This material is available free of charge via the Internet at <http://pubs.acs.org>.

(35) Canales, C. R.; Zimmer, M. *J. Mol. Struct.* **1991**, *245*, 341–347.